Geophys. J. Int. (1999) **137,** 149–158

Effects of superficial layers on coseismic displacements for a dip-slip fault and geophysical implications

R. Cattin,* P. Briole, H. Lyon-Caen,† P. Bernard and P. Pinettes
Institut de Physique du Globe de Paris, Département de sismologie, UMR CNRS 7580, *France*

Accepted 1998 October 27. Received 1998 October 2; in original form 1997 October 7

SUMMARY

We study the effect of a superficial layer overlying a half-space on the surface displacements created by a dip-slip dislocation on a planar rectangular fault using a 2-D finite element model. The effect of the density and Poisson's ratio is negligible. On the other hand, the contrast in Young's modulus between the top layer and the half-space below significantly affects the modelled coseismic displacements. The horizontal displacements are more sensitive than the vertical displacements to the existence of the top layer. Near the fault, a low-rigidity layer with a Young's modulus of 10 GPa can increase the horizontal displacements by up to 40 per cent. An analytical 3-D half-space model is used to interpret this effect in terms of an 'equivalent' homogeneous model. The presence of a top layer can be partly simulated in a homogeneous half-space by perturbing the depth and the slip on the fault from their 'real' values to 'equivalent' values. For a given displacement field observed at the surface, the perturbations in fault depth and slip can reach 1 km and 25 per cent respectively. The fault dip angle is not model-dependent. We conclude that for the accurate estimation of fault depth and slip from coseismic geodetic data, rigidity contrasts existing within the upper crust must be taken into account. Not taking into account the effect of an existing low-rigidity layer also leads to an underestimation of seismic moment release. This may in part be the cause of apparent discrepancies between seismic and geodetic moment releases in particular areas such as the Gulf of Corinth, Greece.

Key words: coseismic displacements, crustal structure, elastic dislocation, normal-faulting earthquakes, Gulf of Corinth.

INTRODUCTION

A dislocation buried in an elastic half-space (Okada 1985, 1992) is a simple model that has often been used to explain most observed coseismic displacements, in agreement with seismological observations (e.g. Marshall *et al.* 1991; Hudnut *et al.* 1994; Ruegg *et al.* 1996). The fault parameters are usually obtained by inverting coseismic displacement assuming a homogeneous half-space.

Today, the availability of data from dense GPS networks and Interferometric Synthetic Aperture Radar (InSAR) images provides a higher spatial coverage and more accurate observations of the coseismic deformations. The interpretation of these higher-quality data requires refinements of the standard model used to simulate the coseismic displacements to be made. In particular, the effect of the rheological parameters of the crust on the modelled displacements has seldom been estimated (Roth 1990; Arnadottir *et al.* 1991; Ma & Kusznir 1994; Savage 1998). Recently, Sabadini & Vermeersen (1997) have shown that the elastic stratification of the lithosphere may have a large influence on coseismic displacement calculated for a deep source. In this paper we analyse the effect of a layer at the top of the upper crust on a shallow normal-faulting earthquake using analytical and numerical modelling. This is a common problem as normal-faulting earthquakes often occur within or at the edges of thick sedimentary basins. Our modelling uses the geometry of the Gulf of Corinth, where Bernard *et al.* (1997) have shown that the geodetic data associated with the Ms=6.2 1995 Aigion earthquake are better explained when a superficial low-rigidity layer is included in the model.

In the first part of this paper, we use a 2-D finite element layered model (LM) to calculate the coseismic displacements associated with a dip-slip fault buried in an elastic half-space overlain by a superficial layer. We use this direct 2-D layered

* Now at: Laboratoire de Géophysique, Bruyères-le-Châtel, France. E-mail: cattin@ldg.bruyeres.cea.fr
† Now at: École Normale Supérieure, Département de Géologie, URA CNRS 1316, France.

model to quantify, for various dip angles of the fault, the effects of rheological parameters and thickness of the top layer on the modelled displacements. In the second part, we discuss how these effects can bias the interpretation in terms of fault parameters when a homogeneous half-space model is assumed (e.g. Okada 1985). Using a given set of surface displacements obtained from the LM, we use an inversion algorithm based on Okada's 3-D analytic half-space solution (HM) to recover 'equivalent' fault parameters that we compare to the initial values. We quantify the departure from the initial values by modelling the coseismic displacements within this homogeneous half-space. Finally, we discuss some geophysical implications for the seismic deformation calculated by summing seismic moment tensors under the assumption of a homogeneous seismogenic layer (e.g. Jackson & McKenzie 1988).

MODELS

Presentation of the models

To calculate the coseismic displacements associated with slip on a buried fault in a LM, we use a finite element code (Hassani 1994) first developed to calculate quasi-static strain of an elasto-viscoplastic discontinuous media. This code uses an explicit finite difference scheme coupled with a dynamic relaxation method to solve 2-D steady-state thermomechanical problems. In this study, space is meshed with 8000 triangular elements. In order to analyse the effects of the superficial layer on the coseismic displacements at the surface, we use a simple LM parametrization (Fig. 1a). The Earth's surface is considered as a stress-free boundary, and in order to keep the structure stable the nodes along the other boundaries are held fixed in the normal direction. We consider a constant dislocation u of 1 m on a 10 km wide fault ($W = 10$ km) with dip angle α. The fault is entirely located within the elastic half-space which is overlain by a top layer of thickness h. The fault ends at $z = 3$ km below the free surface. The rheological parameters of the half-space are fixed: the density ρ' is 2800 kg m^{-3}, the Poisson's ratio ν' is 0.27 and the Young's modulus E' is 10^{11} Pa.

The horizontal and vertical displacements calculated with the LM are then inverted using the HM. For the inversion, we use a code (Briole *et al.* 1986) based on the least-squares minimization developed by Tarantola & Valette (1982). The forward analytical model assumes a uniform dislocation u on a rectangular fault plane (L, W, z, α) in an elastic homogeneous half-space (Okada 1985) (Fig. 1b) .

Validation of the approach

We first compare our 2-D calculations to Savage's (1998) results obtained using an exact elastic solution in the form of Fourier integrals for an edge dislocation in a layered model. The comparison for a vertical dip-slip fault buried in a half-space overlain by a 5 km thick low-rigidity layer is shown in Fig. 2. The agreement between the two calculations is very good (the maximum discrepancy is less than 0.5 per cent of the dislocation u) and validates our 2-D calculations.

The second step is to intercalibrate our 2-D and 3-D calculations. For this, we invert the vertical and horizontal displacements calculated in a 2-D homogeneous half-space for

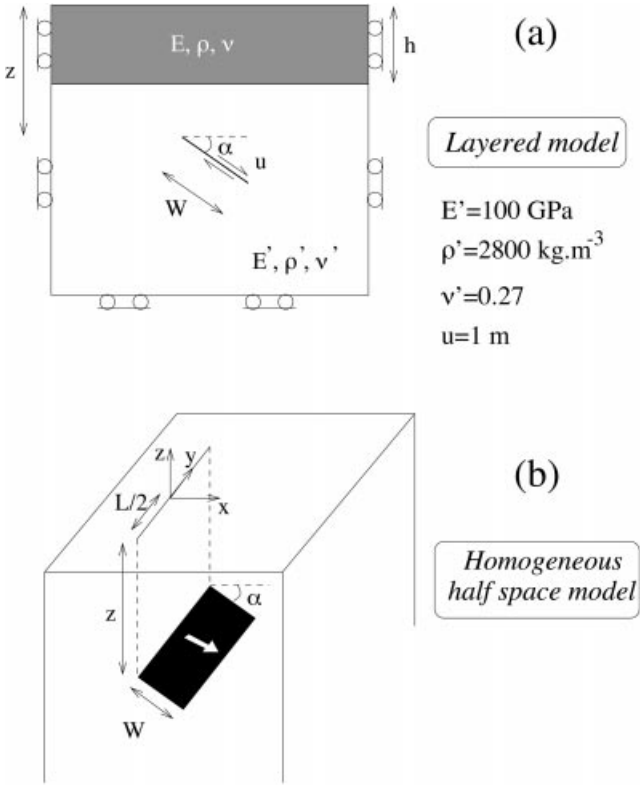

Figure 1. (a) 2-D dislocation model in a layered half-space with an elastic thin layer overlying an elastic half-space (LM). We impose a constant dislocation $u = 1$ m on a fault with a dip angle α, a top depth $z = 3$ km and a width $W = 10$ km. E, ρ, ν and h are the Young's modulus, the density, the Poisson's ratio and the thickness of the top layer, respectively; E', ρ', ν' are the Young's modulus, the density and the Poisson's ratio of the half-space, respectively. (b) 3-D dislocation model in a homogeneous half-space (HM) used to invert the coseismic displacements calculated with the LM. W is fixed at 10 km and $L/W \sim 3$ in the calculations (see text for discussion), while z, u and α are left free.

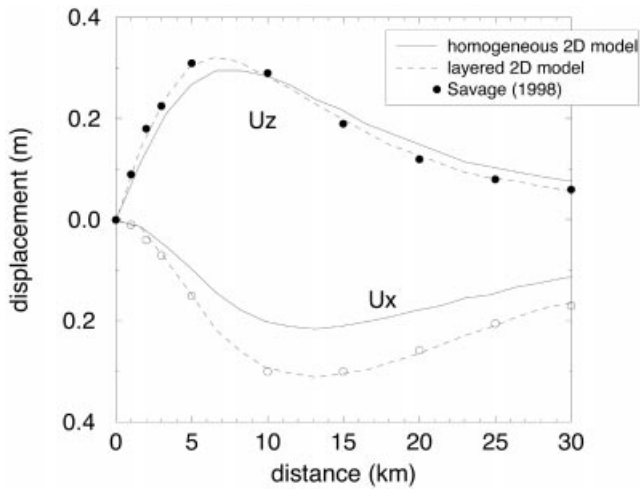

Figure 2. Vertical and horizontal coseismic displacement for a vertical dip-slip fault in a 2-D homogeneous (solid line) and a 2-D layered model (dashed line) calculated with our approach and by Savage (1998) (plotted points). The fault extends from a depth of 9 to 19 km. The top layer of the model has the following parameters: $E/E' = 0.25$, $\nu = \nu' = 0.25$, $u = 2$ m and $h = 5$ km.

a given fault geometry to find the 'equivalent' 3-D fault geometry. Fig. 3 displays the results for an initial fault defined by $u=1$ m, $W=10$ km, $z=3$ km and $\alpha=40°$. In the inversion, W is fixed and u, z, α and L are free. The equivalent 3-D model leads to similar vertical and horizontal displacements and corresponds to values of u, z and α which differ by less than 0.25, 3 and 1 per cent respectively from the initial model. However, the ratio L/W determined in the inversion is ~ 3. The fault is not infinitely long because the 2-D calculations are made in a finite box (300 km long) with constraints of no horizontal displacement on the borders. We show in Fig. 4(a) that it is only for $L/W \geq 10$ that the calculated vertical and horizontal displacements become very close to true 2-D calculations. The variations of L/W with respect to the box size for the fault geometry described above indicate that to reach the condition $L/W \geq 10$ we should use a 600 km long box (Fig. 4b). Because the space is meshed with elements of a constant size, we could not use such a large box and had to restrain our calculations to a 300 km long box corresponding to $L/W \sim 3$. As discussed above, all other parameters of the fault model are accurately retrieved; it is these parameters that we are interested in.

PARAMETRIC STUDY OF THE EFFECT OF THE LOW-RIGIDITY TOP LAYER ON THE COSEISMIC DISPLACEMENTS

In this part, we use the LM to study separately the influence of the thin layer's parameters (ρ, ν, E and h) and the effects of the fault geometrical parameters (α) on the coseismic displacements.

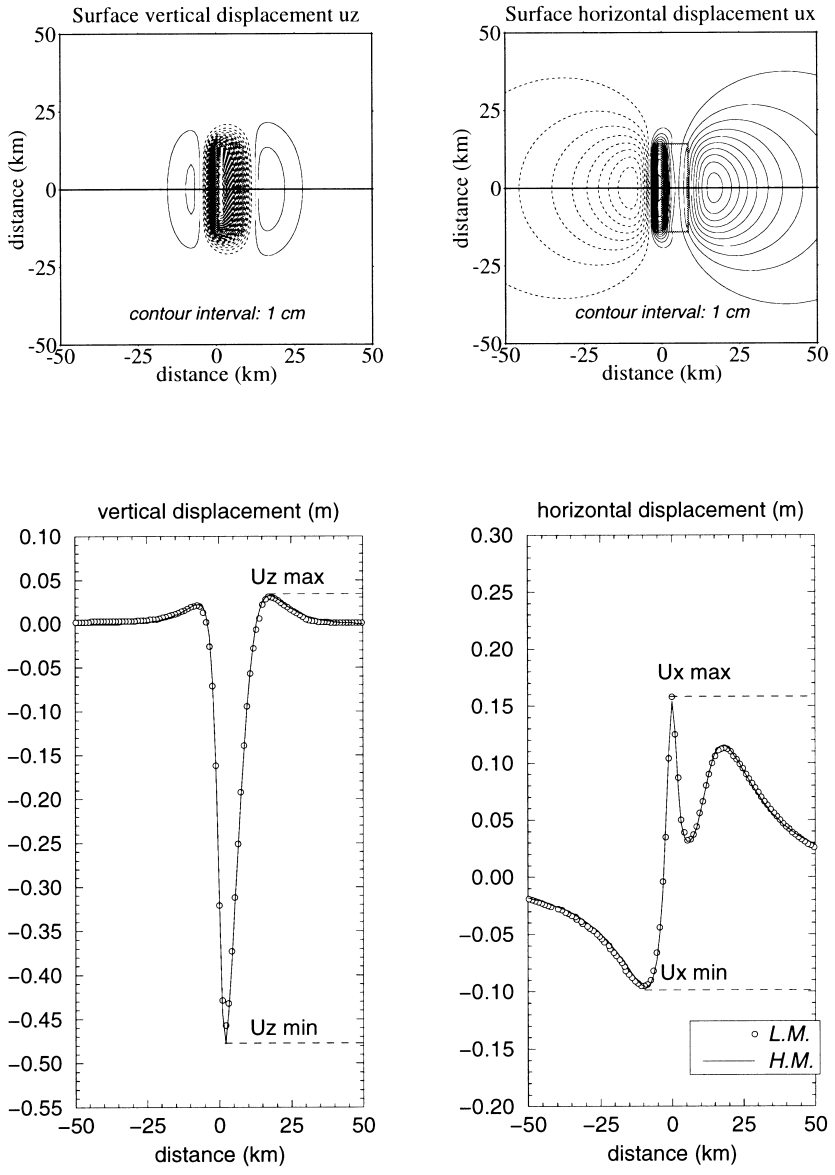

Figure 3. (Top) Map of the surface coseismic displacements calculated with the HM. The rectangle is the fault projected at the surface. The solid line gives the cross-section direction perpendicular to the length of the fault. (Bottom) Comparison of displacements calculated with the LM without top-layer rigidity (open circles) with displacements obtained by inversion using the HM (solid line) with a fault length $L=28.2$ km, for an initial fault defined by $u=1$ m, $W=10$ km, $z=3$ km and $\alpha=40°$.

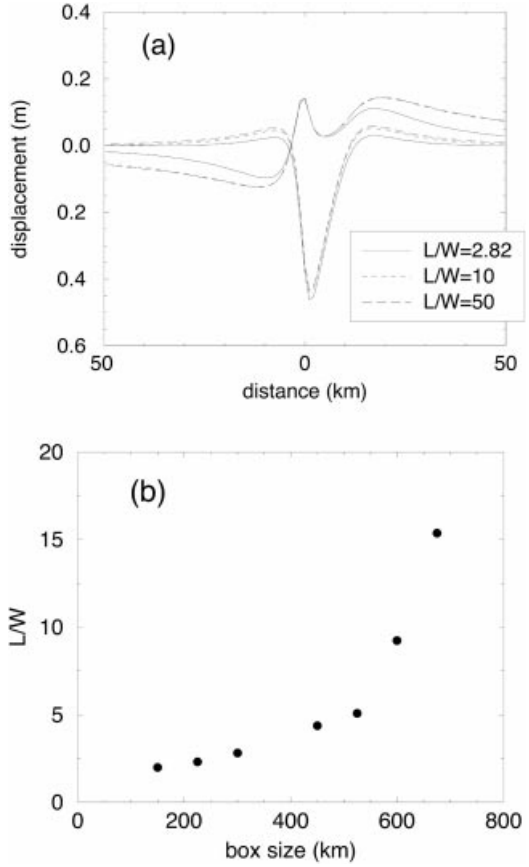

Figure 4. (a) Influence of the length of the fault on the horizontal and vertical coseismic displacements. For $L/W \geq 10$, the 3-D solution is equivalent to the 2-D solution. (b) Effects of the size of the finite element model (maximal distance between the fault and the boundaries) on the fault length L calculated in the HM. When the box size used in the 2-D calculation increases, L becomes semi-infinite (L>>W). $W = 10$ km.

Rheological parameters

In a first set of models, we study the effect of the rheological parameters of the top layer: the density contrast $\delta\rho = \rho - \rho'$, the Poisson's ratio contrast $\delta\nu = \nu - \nu'$ and the Young's modulus ratio $\delta E = E/E'$ between the top and the bottom layers. We make the slip on the fault, u, 1 m, the thickness of the top layer, h, 2 km, the depth of the upper edge of the fault, z, 3 km, the dip angle, α, 40° and the width of the fault, W, 10 km.

The density contrast between the top layer and the medium below has no effect (< 0.1 per cent) on the coseismic displacements when it ranges from 0–0.5 kg m^{-3}. This is consistent with the conclusion of Cohen (1994) which shows that the density contrast between the crust and the mantle produces only minor changes in the calculated surface deformations during the seismic cycle.

We now introduce a Poisson's ratio ν, ranging from 0.01–0.49. The difference in the coseismic displacements reaches 10 per cent. Nevertheless, for most rocks ν ranges from 0.2–0.3, and, like Ma & Kusznir (1995), we find that in this range the Poisson's ratio contrast produces only minor variations (< 5 per cent) in the calculated surface deformations.

Finally, we show in Fig. 5 that the surface displacements, mainly the horizontal ones, are sensitive to the Young's modulus. The measured ratio of the Young's modulus between consolidated or unconsolidated sedimentary rocks and granite ranges from 0.1–0.7 (e.g. Jaeger & Cook 1979; Blangy *et al.* 1993). When the ratio of the Young's modulus between the half-space and the thin layer (E/E') decreases from 1 to 0.1, the horizontal displacements near the fault increase by 40 per cent. This sensitivity of the horizontal coseismic displacements is not linear with E/E'. When (E/E') decreases from 0.1 to 0.01 the variation of horizontal displacements is small (< 10 per cent). When E/E' is small (≤ 0.1) the horizontal surface displacements tend to mimic the deformation at the depth of the interface between the two layers (the low-rigidity layer passively follows the underlying deformation).

In conclusion, the effects of density contrasts and Poisson's ratio (ranging from 0.2–0.3) are negligible. The only parameter that has a significant effect (> 10 per cent) on the modelled coseismic displacements is the contrast of the Young's modulus between the top layer and the half-space below.

Geometrical parameter: thickness of the low-rigidity layer and fault dip angle

In the following, we assume that $\delta\rho = 0.3$ kg m^{-3}, $\delta\nu = 0$ and $E/E' = 0.1$ and we study the influence of the thickness h of the low-rigidity layer. The vertical displacements are not distorted (< 10 per cent) when h increases from 0 to 1, 2 and 3 km (Fig. 6). In contrast, h has a large influence on the surface coseismic horizontal displacements. Near the fault, the horizontal displacements increase by 20 and 45 per cent when h increases from 0 to 1 km and 0 to 3 km respectively.

The last parameter studied in this section is the fault dip angle α. We use a thickness h of 2 km. Again, the vertical displacement is mostly unchanged (< 6 per cent) when α ranges from 20°–60° with or without the low-rigidity layer (Fig. 7). Whatever the dip is, the horizontal displacements near the fault are sensitive (> 30 per cent variation) to the presence of the low-rigidity layer.

In order to better compare the influence of E, α and h, we use the normalized displacement parameter

$$Ui_{\text{norm}} = \frac{\delta Ui - \delta Ui_{\text{homogeneous}}}{\delta Ui_{\text{homogeneous}}}, \quad (1)$$

where i is the displacement component and $\delta Ui = Ui_{\max} - Ui_{\min}$ (see Fig. 3). The sensitivity of normalized displacements to the low-rigidity layer is almost the same for α ranging from 20°–60° (Fig. 8). In contrast, the normalized horizontal displacements range from 0 to ~40 per cent when E/E' decreases from 1 to 0.1, and they range from ~20 to 45 per cent when the thickness of the low-rigidity layer increases from 1 to 3 km.

Furthermore, as we have already shown, the horizontal displacements are more sensitive to the presence of the low-rigidity layer than the vertical component. This behaviour is also mentioned by Savage (1998). In order to explain this result we calculate u_x and u_z versus depth in the HM with the parameters described above ($u = 1$ m, $W = 10$ km, $L = 28.2$ km, $z = 3$ km, $\alpha = 40°$). There is no vertical gradient for u_z in the upper part of the model, whilst u_x exhibits strong vertical gradients, which makes u_x potentially very sensitive to near-surface structure (Fig. 9). The horizontal component is thus more sensitive to shallow Young's moduli layering than the vertical component.

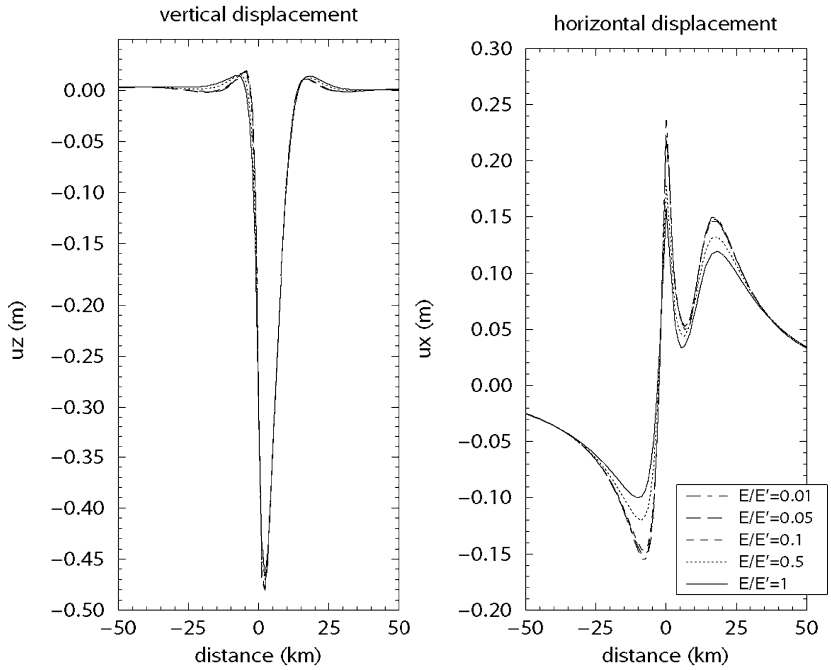

Figure 5. Effect of the Young's modulus of the top layer on the vertical and horizontal coseismic displacements. The Young's modulus of the lower half-space (E') is 100 GPa.

HOMOGENEOUS HALF-SPACE 'EQUIVALENT' MODEL

In order to quantify the 'errors' made in fault geometry and slip due to the assumption of homogeneity we calculate the displacements due to a dislocation embedded in a layered half-space (LM) and we interpret it in the context of an equivalent homogeneous half-space (HM), as is usually done. To do this, we invert with the HM the horizontal and vertical displacements generated previously with the LM to calculate u, z and α.

We start our inversions using as *a priori* values the parameters of the LM ($u=1$ m, $z=3$ km, $\alpha=40°$). We make the

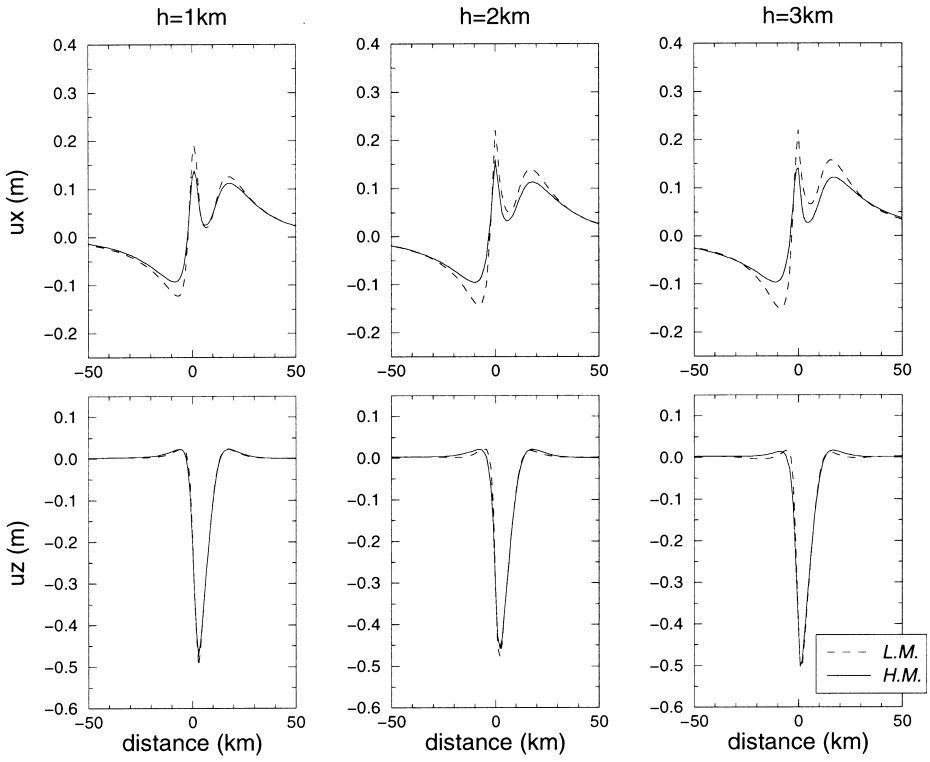

Figure 6. Effect of the thickness h of the low-rigidity layer on the horizontal (u_x) and vertical (u_z) coseismic displacements with $\alpha=40°$ and $E/E'=0.1$.

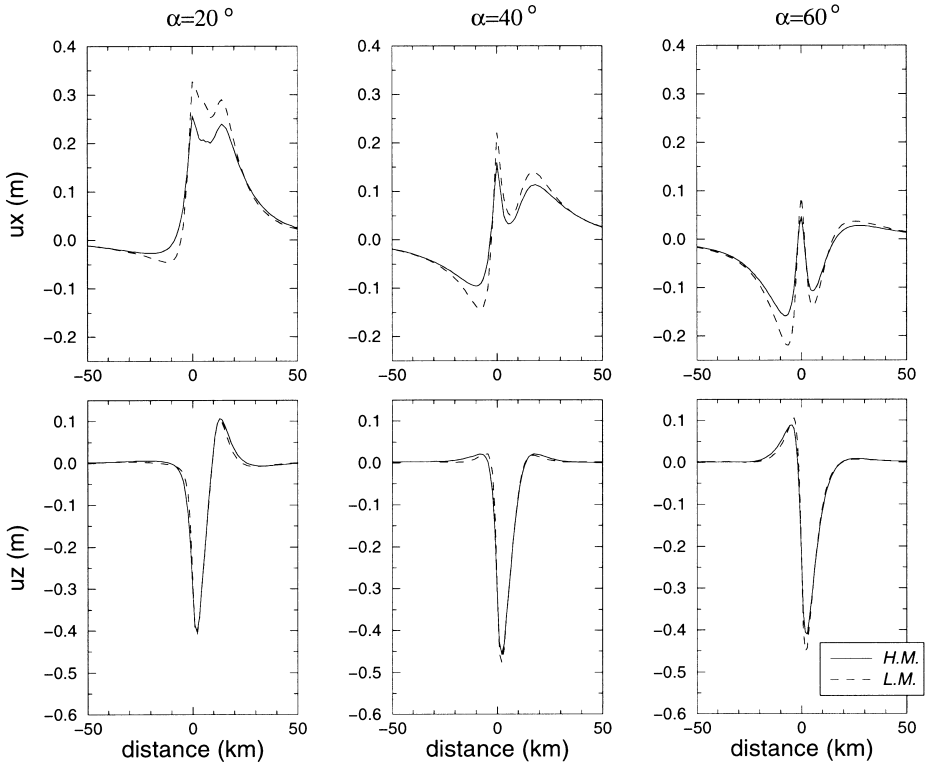

Figure 7. Effect of the dip angle of the fault on the horizontal (u_x) and vertical (u_z) coseismic displacements with $h=2$ km and $E/E'=0.1$.

fault width 10 km and the fault length 28.2 km, as determined by the inversion of the displacements calculated with the LM without any low-rigidity top layer (see the 'models' section). Two sets of inversions are made, the first with the two components of the displacement and the second with only the horizontal displacements since these are often the only components available .

For all models, we observe that the inverted dip angle matches the 'true' dip angle of the LM. The only parameters sensitive to the presence of the low-rigidity top layer are the

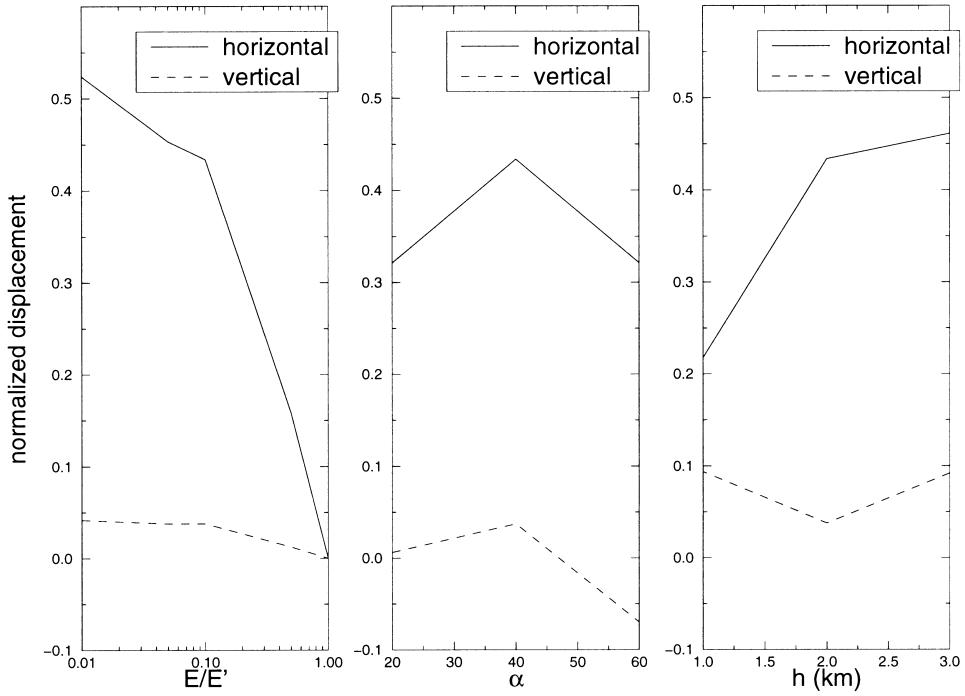

Figure 8. Normalized displacement variations with E, α and h. The low-rigidity layer has a larger influence on the horizontal displacements than on the vertical displacements.

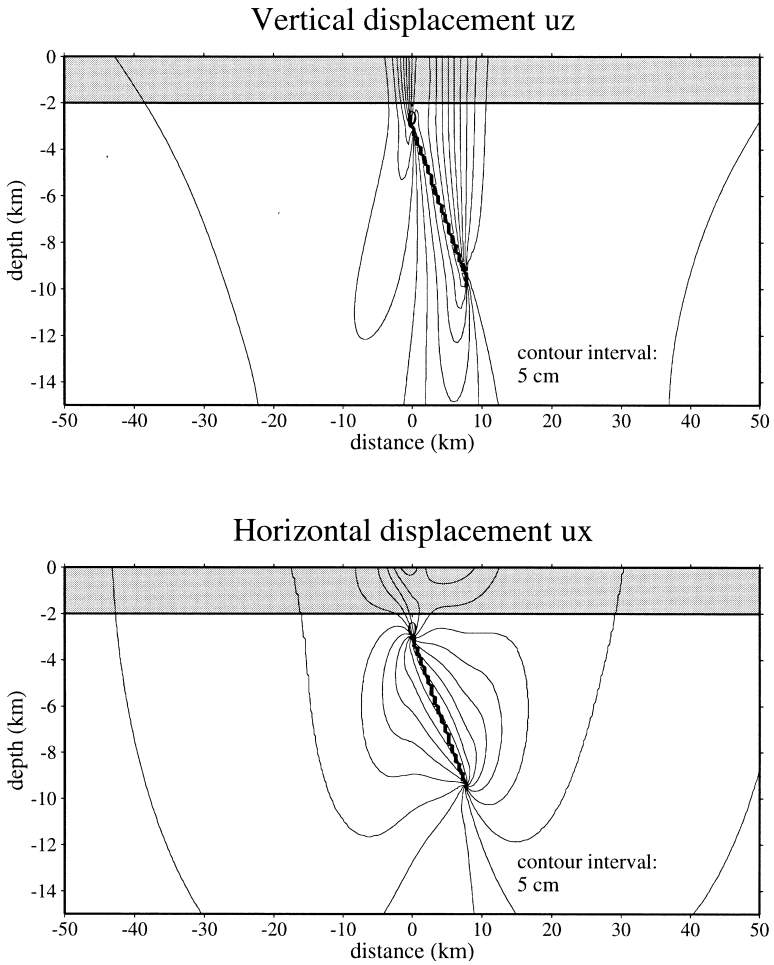

Figure 9. Distribution of the vertical (top) and horizontal (bottom) components of the displacement with depth, calculated without a low-rigidity layer ($u=1$ m, $W=10$ km, $z=3$ km, $\alpha=40°$). The vertical displacements exhibit no vertical gradient, whilst the horizontal displacements exhibit a vertical gradient. This difference can explain the different sensitivities of the two components to the presence of a thin low-rigidity layer.

depth z of the upper edge of the fault and the slip u on the fault. Thus, for each model we study the effect of the low-rigidity layer on these parameters by using $\delta z = z_{\text{inverted}} - z_{\text{true}}$ and the slip variation

$$\frac{\delta u}{u} = \frac{u_{\text{inverted}} - u_{\text{true}}}{u_{\text{true}}}, \tag{2}$$

where 'true' means 'as used in the LM'. In the reference model, the following parameters are used: $E=10$ GPa, $h=2$ km and $\alpha=40°$.

When the Young's modulus of the low-rigidity layer varies between 50 and 5 GPa ($0.5 > E/E' > 0.05$) (Fig. 10), $\delta u/u$ does not change (< 3 per cent) and δz decreases from -345 to -750 m. Moreover, the half-space equivalent model cannot fully explain the horizontal displacements near the projection of the fault. The discrepancy is ~ 20 per cent. When we invert only the horizontal displacements, this discrepancy becomes very low (< 2 per cent) and $\delta u/u$ varies between 7 and 17 per cent, and δz decreases from -550 to -255 m. This behaviour is consistent with the results of Savage (1998), which suggest that 'the neglect of the low-modulus layer in the edge dislocation problem causes one to underestimate the depth of the dislocation'.

We now study the effect of the thickness of the top layer. The fault depth is the only parameter that is sensitive to the thickness (Fig. 11). δz varies between -320 and -860 m when the thickness increases from 1 to 3 km. The 'error' on the slip is small and independent of the thickness ($\delta u/u < 3$ per cent). However, $\delta u/u$ becomes sensitive to the thickness of the low-rigidity layer when we invert only the horizontal displacements.

The last parameter studied is the dip angle. We see that δz varies between -770 and -530 m with two components, and between -850 and -310 m with only the horizontal component when the dip angle ranges from 20°–60° (Fig. 12). Again $\delta u/u$ is sensitive to the fault dip angle when we use only the horizontal displacements, and reaches ~ 25 per cent for $\alpha=60°$.

CONCLUSIONS

Our parametric study has shown that the only rheological parameter that has a significant effect on coseismic displacements is the Young's modulus ratio E/E' between the upper layer and the underlying half-space. Although vertical displacements are not affected, calculated horizontal

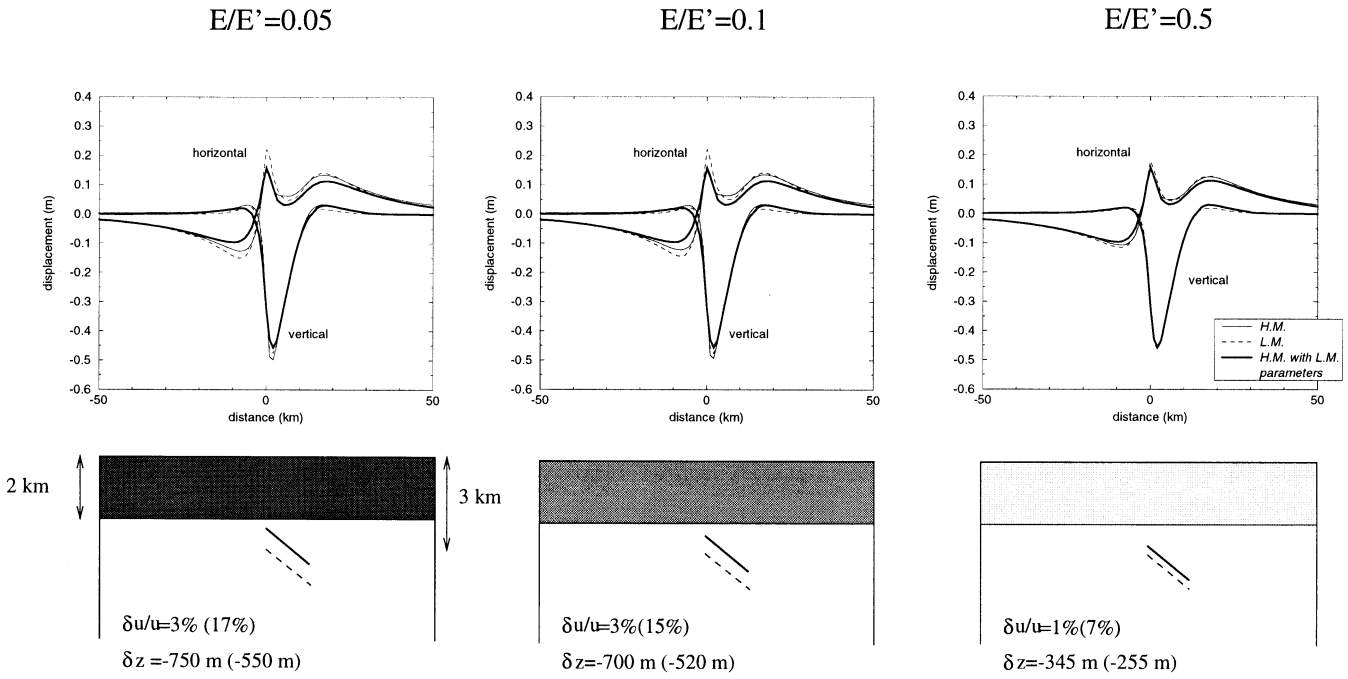

Figure 10. Equivalent homogeneous half-space for various Young's modulus contrasts with $\alpha = 40^\circ$ and $h = 2$ km. (Top) The coseismic displacements are calculated with the 'equivalent' HM (solid line), with the LM (dashed line) and with the HM but with the LM parameters (thick solid line). The 'equivalent' model is determined by using the two displacement components. (Bottom) The solid line indicates the fault position in the 'equivalent' HM and the dashed line that in the LM. $\delta u/u$ and δz are the slip variation and the depth variation calculated with two components; the values for the horizontal component only are given in brackets.

displacements may vary by more than 40 per cent when E/E' varies from 1 to 0.1.

Using a homogeneous half-space to interpret the coseismic displacements leads to shallower faults than in reality in all cases and tends to overestimate the slip by 10–20 per cent when horizontal displacements alone are considered. This is consistent with Savage's (1998) conclusions. Still, in most cases the homogeneous equivalent model is not able to explain simultaneously vertical and horizontal displacements, and close to the fault discrepancies of generally 10–20 per cent remain.

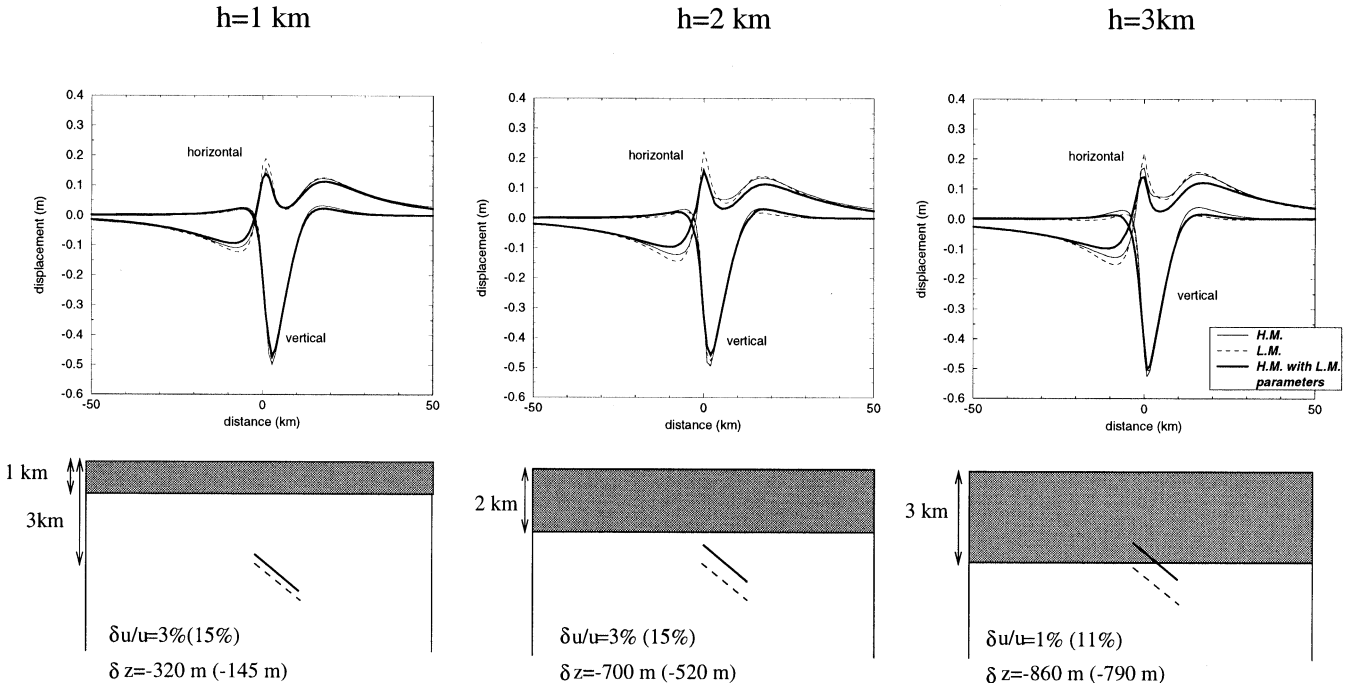

Figure 11. Equivalent homogeneous half-space for various thicknesses of the low-rigidity layer with $\alpha = 40^\circ$ and $E/E' = 0.1$. See Fig. 10 caption.

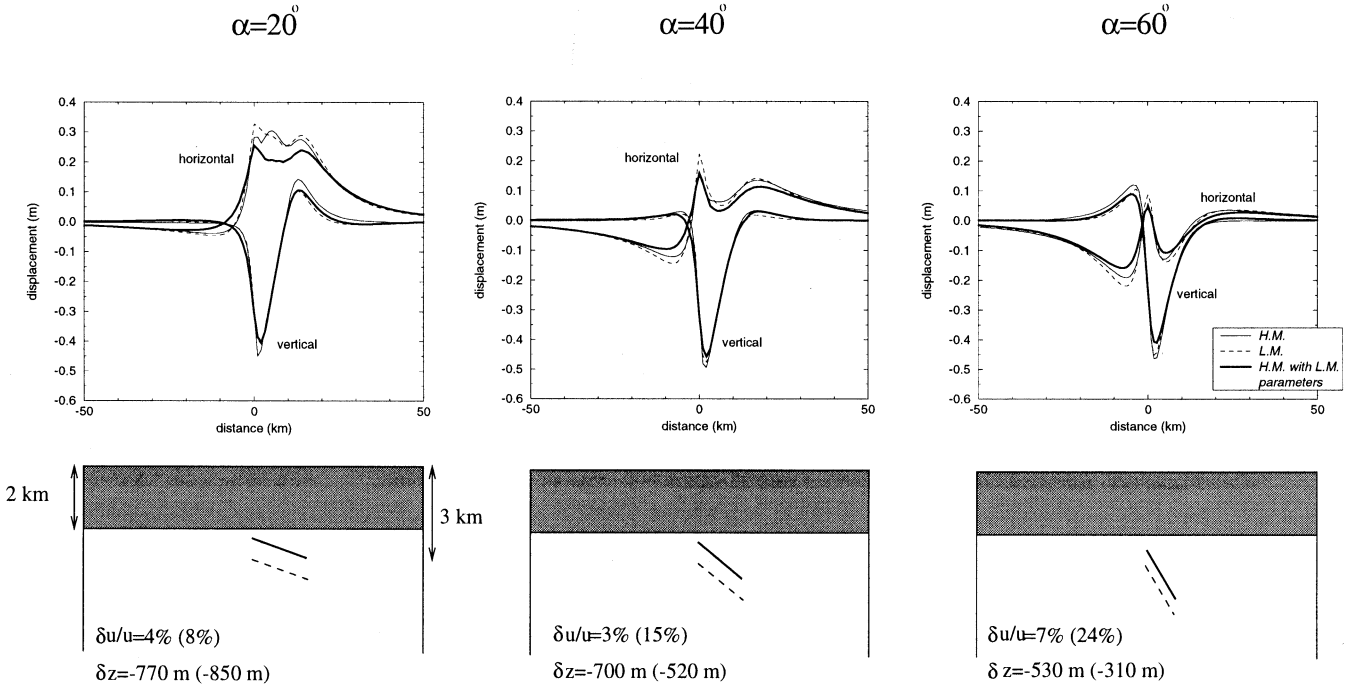

Figure 12. Equivalent homogeneous half-space for faults of various dip angles with $E/E'=0.1$ and $h=2$ km. See Fig. 10 caption.

The largest depth variations ($\sim$1 km) are obtained for shallow-dipping faults (Fig. 12) and when the thickness of the low-rigidity layer is high (Fig. 11). The 1995 Aigion earthquake in the Corinth rift occured on a 33° dipping normal fault with a centroid depth of 7.2 km. In this case Bernard *et al.* (1997) had to lower the depth of the fault by 2 km to explain the observed horizontal displacements. This is about twice the maximal value obtained with the examples studied here. This may be due to a locally thicker sedimentary layer or to a greater depth of the fault than we have assumed in our calculations. In any case, the fact that the equivalent homogeneous model in general does not fully explains horizontal and vertical displacements stresses the need for computing dislocations in a 3-D layered medium.

The behaviour of coseismic displacements shown here may have some important consequences on conclusions derived from seismic moment tensor summations (e.g. Ekström & England 1989; Jackson & McKenzie 1988). In these studies, a key parameter in estimating the regional seismic deformation is the seismogenic layer thickness or elastic thickness in which the seismic deformation is confined. This thickness is usually taken as the maximum depth of the crustal seismicity in a given area. The calculations presented in this paper show that the apparent thickness of the seismogenic layer depends on the thickness of the top low-rigidity layer, if present. In the presence of well-developed sedimentary basins, the underestimation of horizontal displacements created by a given earthquake can reach $\sim$40 per cent (see Fig. 5). In the Gulf of Corinth area, estimations of seismic moment rates and geodetic rates of deformation differ by a factor of about 2 (Ambraseys & Jackson 1990; Papazachos & Kiratzi 1992; Clarke *et al.* 1997). We suggest that part of this discrepancy is due not to a strain energy accumulation that will eventually be released in large earthquakes (Clarke *et al.* 1997) or to aseismic deformation (Papazachos & Kiratzi 1992), but rather to the presence of a thick sedimentary basin that makes the seismogenic layer thinner than assumed in previous strain-rate calculations. The role of superficial layers may be important in other areas such as the Basin and Range Province, where recent GPS measurements indicate unexpected rapid deformation rates (Martinez *et al.* 1998).

ACKNOWLEDGMENTS

We are grateful to R. Armijo, J. B. de Chabalier and J. C. Ruegg for useful discussions about the structure of the Gulf of Corinth. We would like to thank Y. Okada for having provided us with his Fortran routines for his 1992 paper and J. Chéry and R. Hassani for the finite element code. We would also like to thank R. Sabadini and two anonymous reviewers for their helpful comments on the original version of the manuscript.

REFERENCES

Ambraseys, M.N. & Jackson, J.A., 1990. Seismicity and associated strain of central Greece between 1890 and 1988, *Geophys. J. Int.*, **101,** 663–708.

Arnadottir, T., Segall, P. & Delaney, P., 1991. A fault model for the 1989 Kilauea south flank earthquake from leveling and seismic data, *Geophys. Res. Lett.*, **18,** 2217–2220.

Bernard, P. *et al.*, 1997. The Ms=6.2, June 15, 1995 Aigion earthquake (Greece): evidence for low angle normal faulting in the Corinth rift, *J. Seism.*, **1,** 131–150.

Blangy, J.P., Strandenes, S., Moos, D. & Nur, A., 1993. Ultrasonic velocities in sand—revisited, *Geophysics,* **58,** 344–356.

Briole, P., De Natale, G., Gaulon, R., Pingue, F. & Sparca, R., 1986. Inversion of geodetic data and seismicity associated with the Friuli earthquake sequence (1976–1977), *Ann. Geophys.*, **4,** 481–492.

Clarke, P. *et al.,* 1997. Geodetic estimation of seismic hazard in the Gulf of Corinthos, *Geophys. Res. Lett.,* **24,** 1303–1306.

Cohen, S.C., 1994. Evaluation of the importance of model features for cyclic deformation due to dip-slip faulting, *Geophys. J. Int.,* **119,** 831–841.

Ekström, G. & England, P., 1989. Seismic strain rates in regions of distributed continental deformation, *J. geophys. Res.,* **94,** 10 231–10 257.

Hassani, R., 1994. Modélisation numérique de la déformation des systémes géologiques, *Thèse,* Université Monpellier II, France.

Hudnut, K.W. *et al.,* 1994. Co-seismic displacements of the 1992 Landers Earthquake sequence, *Bull. seism. Soc. Am.,* **84,** 625–645.

Jackson, J. & McKenzie, D., 1988. The relationship between plate motions and seismic moment tensors, and the rates of active deformation in the Mediterranean and Middle East, *Geophys. J.,* **93,** 45–73.

Jaeger, J.C. & Cook, N.G., 1979. *Fundamentals of Rock Mechanics,* Chapman & Hall, London.

Ma, X.Q. & Kusznir, N.J., 1994. Effects of rigidity layering, gravity and stress relaxation on 3-D subsurface fault displacement fields, *Geophys. J. Int.,* **118,** 201–220.

Ma, X.Q. & Kusznir, N.J., 1995. Coseismic and postseismic subsurface displacements and strains for a dip-slip normal fault in a three-layer elastic-gravitational medium, *J. geophys. Res.,* **100,** 12 813–12 828.

Marshall, G.A., Stein, R.S. & Thatcher, W., 1991. Faulting geometry and slip from co-seismic elevation changes: the 18 October 1989, Loma Prieta, California, earthquake, *Bull. seism. Soc. Am.,* **81,** 1660–1693.

Martinez, L., Meertens, C. & Smith, R., 1998. Rapid deformation rates along the Wasatch fault zone, Utah from first GPS measurements with implications for earthquake hazard, *Geophys. Res. Lett.,* **25,** 567–570.

Okada, Y., 1985. Surface deformation due to shear and tensile faults in a half-space, *Bull. seism. Soc. Am.,* **75,** 1135–1154.

Okada, Y., 1992. Internal deformation due to shear and tensile faults in a half space, *Bull. seism. Soc. Am.,* **82,** 1018–1040.

Papazachos, C.B. & Kiratzi, A.A., 1992. A formulation for reliable estimation of active crustal deformation and its application to central Greece, *Geophys. J. Int.,* **111,** 424–432.

Roth, F., 1990. Subsurface deformations in a layered elastic half-space, *Geophys. J. Int.,* **103,** 147–155.

Ruegg, J.C. *et al.,* 1996. The Mw = 8.1 Antofagasta (North Chile) earthquake of July, 1995: first results from teleseismic and geodetic data, *Geophys. Res. Let.,* **23,** 917–920.

Sabadini, R. & Vermeersen, L.L.A., 1997. Influence of lithospheric and mantle stratification on global post-seismic deformation, *Geophys. Res. Let.,* **24,** 2075–2078.

Savage, J.C., 1998. Displacement field for an edge dislocation in a layered half-space, *J. geophys. Res.,* **103,** 2439–2446.

Tarantola, A. & Valette, B., 1982. Generalized non linear inverse problem solved using the least squares criterion, *Rev. Geophys.,* **20,** 219–232.